Precision Medication 2 (2025) 100050

Contents lists available at ScienceDirect

Precision Medication

journal homepage: www.keaipublishing.com/en/journals/precision-medication/

Integrative multi-omics approach for drug repositioning in Alzheimer's disease

Jinna Yang[a,b], Kaimin Guo[a,b], Xiaxia Ren[a,c], Xiaolian Zhang[d], Shuang Zhao[a,b], Jiansong Fang[d], Yu Wei[a,b], Pengcheng Yang[a,b], Wenjia Wang[a,b], Hui Wang[e,*], Yunhui Hu[a,b,*]

[a] Tianjin Tasly Digital Intelligence Chinese Medicine Technology Co., Ltd, Tianjin 300410, China
[b] State Key Laboratory of Chinese Medicine Modernization, Tianjin 300193, China
[c] Tianjin University of Traditional Chinese Medicine, Tianjin 301617, China
[d] Science and Technology Innovation Center, Guangzhou University of Chinese Medicine, Guangzhou 510405, China
[e] Key Laboratory of Molecular Biophysics, Hebei Province, Institute of Biophysics, School of Health Sciences and Biomedical Engineering, Hebei University of Technology, Tianjin 300401, China

ARTICLE INFO

Keywords:
Alzheimer's disease
Drug repurposing
Multi-omics
RGES
C-Map

ABSTRACT

Background: Alzheimer's disease (AD) is a progressive neurodegenerative disorder with an insidious onset, and effective therapeutic agents are urgently needed.
Objective: This study employed a multi-omics integration strategy for drug repurposing against AD.
Methods: Firstly, transcriptomic and proteomic data from AD patients were utilized to identify differentially expressed genes. Potential anti-AD small-molecule compounds were screened by integrating the Reverse Gene Expression Score (RGES) and Connectivity Map (C-Map) approaches with drug-perturbed gene expression profiles from the Library of Integrated Network-Based Cellular Signatures (LINCS), followed by blood-brain barrier (BBB) permeability prediction and structural similarity analysis. Secondly, a drug-disease network was constructed, and Gene Ontology (GO) and Kyoto Encyclopedia of Genes and Genomes (KEGG) pathway enrichment analyses were performed. The therapeutic potential of candidate drugs was further evaluated via network proximity analysis. Finally, in vitro validation was conducted using Okadaic acid (OA) induced SH-SY5Y and Lipopolysaccharide (LPS) induced BV2 cell models to assess cell viability and nitric oxide (NO) levels. This integrated approach provides a novel framework for identifying repurposed drugs with potential efficacy against AD.
Results: Following the collection of omics data, 227 overlapping candidate compounds were identified through two computational approaches. After BBB prediction screening, 104 drugs were selected for subsequent structural similarity analysis and literature/patent review, ultimately leading to the selection of TNP-470 and Terreic acid for validation. Network pharmacology analysis revealed that potential targets of TNP-470 for AD treatment were significantly enriched in neuroactive ligand-receptor interaction, TNF signaling, and AD-related pathways, while anti-AD targets of Terreic acid primarily involved calcium signaling, AD pathway, and cAMP signaling. Network proximity analysis demonstrated significant associations between both candidates and AD. In vitro assays demonstrated that TNP-470 significantly enhanced the viability of OA-induced SH-SY5Y cells at concentrations of 10 μM and 50 μM ($p < 0.01$ and $p < 0.05$, respectively). Additionally, within the concentration range of 0.016–10 μM, TNP-470 markedly inhibited NO production in the LPS-induced BV2 microglial cell model. Terreic acid also promoted the survival of OA-treated SH-SY5Y cells at concentrations ranging from 2 to 50 μM, and significantly reduced nitric oxide (NO) levels at a concentration of 10 μM.
Conclusion: This drug repositioning strategy based on multi-omics integration provides a novel approach for AD therapeutic development, with both TNP-470 and Terreic acid demonstrating anti-AD potential.

*Corresponding authors.
E-mail addresses: huiwang@hebut.edu.cn (H. Wang), tsl-huyunhui@tasly.com (Y. Hu).

https://doi.org/10.1016/j.prmedi.2025.100050
Received 10 June 2025; Received in revised form 13 July 2025; Accepted 16 July 2025
Available online 17 September 2025

Introduction

AD is an insidious-onset, progressive neurodegenerative disorder of the nervous system, categorized as a brain disease caused by damage to neuronal cells in the brain. Clinically, it is characterized by comprehensive dementia manifestations, including memory impairment, aphasia, apraxia, agnosia, visuospatial skill deficits, executive dysfunction, and personality/behavioral changes, imposing severe economic burdens on individuals, families, and society.[1] With the global population aging, the number of AD patients has grown at an alarming rate, with projections estimating that this figure will reach 150 million by 2050.[1–3] The core pathological hallmarks of AD include the accumulation of amyloid plaques and neurofibrillary tangles (NFTs) in the brain, accompanied by synaptic and neuronal damage, which ultimately leads to cognitive impairment.[4] Despite the numerous AD drugs in development, only a limited number have been approved for clinical use in China. Currently marketed treatments primarily include galantamine, rivastigmine, donepezil, memantine, and Sodium oligomannate capsules (GV-971),[5] as well as two anti-amyloid therapeutic agents: aducanumab, lecanemab and donanemab.[6–8] However, these medications only provide symptomatic relief, fail to halt disease progression, and lack robust evidence from high-quality evidence-based medicine.[5] Consequently, the development of highly effective and feasible therapeutic agents for AD remains an urgent priority for patients and healthcare systems worldwide.

Traditional drug development methods are time-consuming, costly, and have a high failure rate. In contrast, drug repurposing is a strategy that uses big data-related technologies to rescreen, combine, or modify existing drugs to discover their previously unknown new applications. Compared with traditional drug development, this approach offers numerous advantages, including lower risk, shorter development cycles, less investment, and faster entry into clinical trials. It is an effective way to accelerate the development of new drugs. Using multi-omics for drug repurposing has emerged as a novel strategy.[9,10] The LINCS perturbs cultured cells through various means (such as small molecules, ligands, microenvironmental changes, CRISPR gene overexpression, and knockdown) and detects transcriptomic data of the perturbed activity, typically across multiple cell types, time points, and doses. This provides a rich data foundation for drug-based repurposing strategies.[11] In recent years, the number of studies on drug repurposing based on the LINCS database has been gradually increased. For example, mifepristone was screened as an anti-AD drug by targeting vesicular glutamate transporter 1 using the LINCS database.[12] Givinostat was identified as a potential therapeutic agent for AD based on the LINCS database.[13] These studies demonstrate that drug screening and repurposing can be effectively conducted based on the specific expression profiles of drugs or diseases. However, to date, no new small-molecule drugs have been launched, and effective treatments for AD remain scarce.

This study employs a multi-omics integration strategy for drug repurposing in AD. Fig. 1 illustrates the research workflow. First, differential genes/proteins were screened based on transcriptomic and

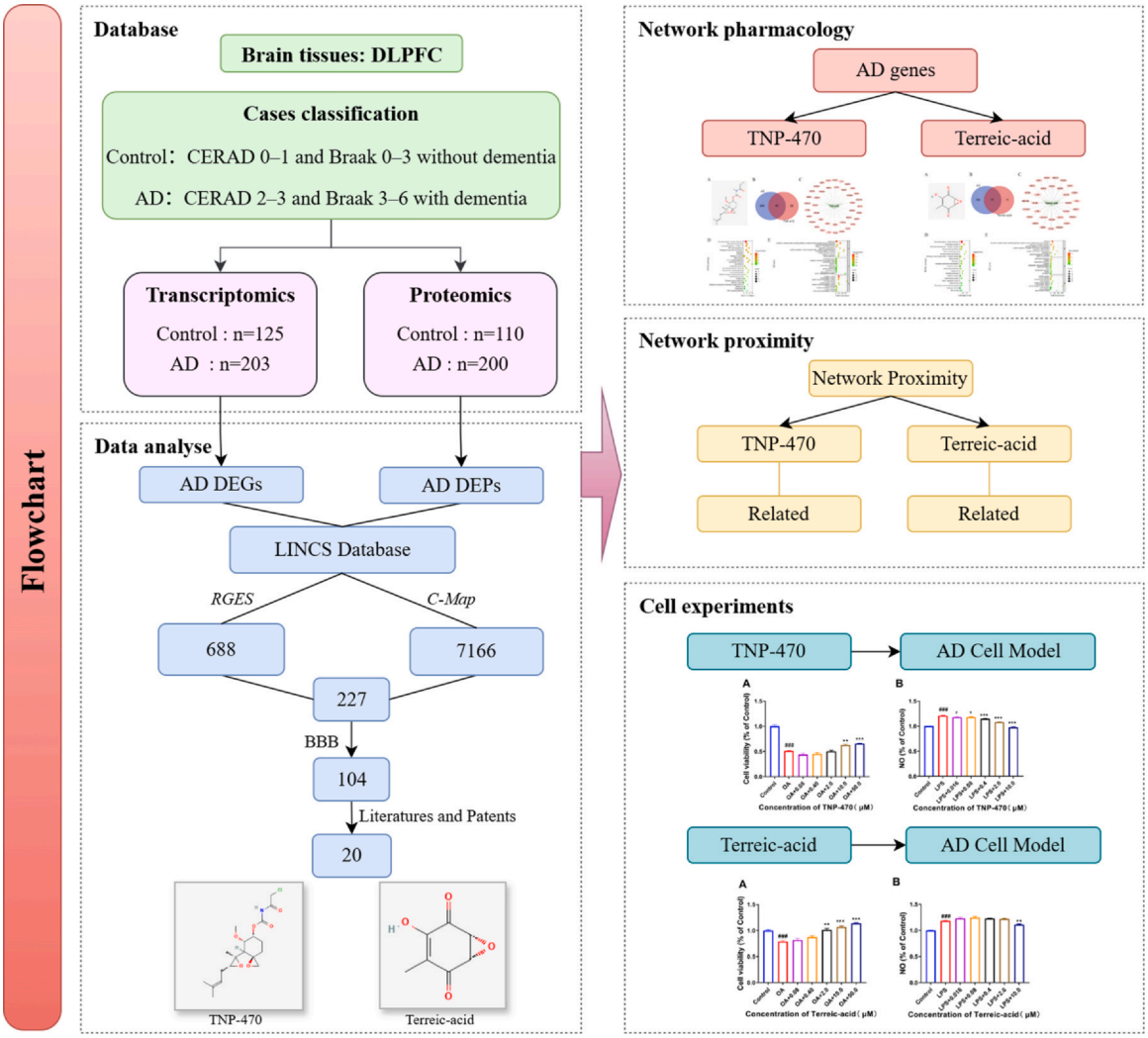

Fig. 1. Flowchart of this study. Screening and validation of drugs based on the reversal relationship of disease and drug-related gene expression profiles. DLPFC: dorsolateral prefrontal cortex; CERAD: Consortium to Establish a Registry for Alzheimer's Disease.

proteomic data from AD patients. Using the RGES method developed by Chen et al.,[14] disease-associated differential genes were computationally compared with gene expression profiles of drug perturbations in the LINCS database to identify potential AD therapeutic candidates. Further analysis utilized the C-Map algorithm,[15] integrating proteomic differential proteins with drug perturbation profiles from LINCS to screen additional candidate drugs. Results from the two methods were cross-validated and compared. Second, target networks of diseases and drugs were collected for network pharmacology analysis and network proximity calculation, assessing the potential efficacy of candidate drugs against AD. Finally, in vitro cell experiments were performed to validate the pharmacodynamic effects of the candidates, leading to the identification of two potential drugs with therapeutic potential for AD.

Materials and methods

Cell lines

The human neuroblastoma cell line SH-SY5Y and the murine microglial cell line BV2 were obtained from the cell bank of the Chinese Academy of Sciences. These cell lines were cultured in Dulbecco's Modified Eagle Medium (DMEM) (Gibco, C11995500BT) supplemented with 10 % fetal bovine serum (FBS) (Vivacell, C04001–500) and 1 % penicillin/streptomycin (PS) (Solarbio, P1400). The cultures were maintained in an incubator with 5 % CO_2 at a temperature of 37 °C.

Cell counting kit-8 (CCK8) assay

CCK8 assay was performed with a CCK8 kit (Solarbio, CA1210) according to the manufacturer's protocol. Briefly, logarithmic-phase SH-SY5Y cells were digested with trypsin(Solarbio, T1320) to obtain a single-cell suspension. And then cells were seeded into 96-well plates at a density of 5×10^3 cells per well in 100 μL of induction medium and categorized into different groups. The model and drug treatment groups received OA (MedChemExpress, HY-N6785) at a concentration of 20 nM, while the blank group did not receive OA or any drugs. Different dosages of TNP-470 (MedChemExpress, HY-101932) or Terreic acid (MedChemExpress, HY-110013) were added to drug treatment groups. After cultured for 24 h, CCK8 detection was performed by adding 10 μL of CCK8 reagent to each well for 1 h before analysis. The absorbance at 450 nm was measured using a Multiskan FC Microplate Reader. Cell proliferation rates were calculated as the absorbance of treated cells compared with an untreated control group.

NO ELISA kit assay

Logarithmic-phase BV2 cells were digested with trypsin (solarbio, T1320) to single-cell suspension and seeded into 96-well plates at a density of 5×10^3 cells per well and categorized into different groups. The model and drug treatment groups received LPS (Sigma, L2880) at a concentration of 1 μg/ml, while the blank group did not receive LPS or any drugs. After cultured for 24 h, cell lysates were centrifuged, and the supernatants were collected. The concentration of NO were measured in the supernatants with ELISA kits (Beyotime, S0021) according to the manufacturer's protocols.

Compilation of drug-induced transcriptomic signatures

Drug transcriptomic profiles were obtained from the LINCS database (https://clue.io/connectopedia/LINCS_C-Map_data), which contains perturbation signatures of FDA-approved drugs or clinical trial compounds across various cell lines.[11] For each drug, the dataset includes transcriptomic responses under different concentrations, treatment durations, and cell line backgrounds, comprising a total of over 66,612 and adjacent normal tissues, using data downloaded from TCGA. We then collected 66,612 compound gene expression profiles, consisting of 12,442 distinct compounds profiled in 71 cell lines (with 83 % of the measurements made primarily in 15 cell lines), using data downloaded from LINCS. Each profile involved the expression measurement of 978 genes, termed 'landmark genes'. The changes in the expression of these landmark genes were computed after compounds were tested.

Collection of omics data in Alzheimer's disease

The transcriptional and proteomic profiles of AD, including differentially expressed genes (DEGs), and Differentially expressed proteins (DEPs), were extracted from brain tissue samples of clinical patients.[16] A total of 328 dorsolateral prefrontal cortex (DLPFC) samples, comprising 125 control and 203 AD cases, were analyzed in this study. All human postmortem DLPFC tissues were obtained from two well-established longitudinal clinical-pathological cohort studies: the Religious Orders Study and Memory and Aging Project (ROSMAP) and the Banner Sun Health Research Institute. Tissue collection was conducted under protocols approved by the institutional review board protocols at each respective institution. Written informed consent was obtained from all participants prior to death, in accordance with ethical guidelines and regulatory requirements. Neuropathological assessment was performed centrally at each institution following standardized and validated criteria. The density of neuritic plaques was evaluated using the scoring system developed by the Consortium to Establish a Registry for Alzheimer's Disease (CERAD), while the distribution and progression of neurofibrillary tangle pathology were assessed using the Braak staging method. Additional neuropathological evaluations were carried out to exclude other common neurodegenerative diseases, based on established consensus diagnostic criteria. Cases with CERAD 0–1 and Braak 0–3 without dementia at last evaluation were defined as control (if Braak equals 3, then CERAD must equal 0) and cases with CERAD 2–3 and Braak 3–6 with dementia at last evaluation were defined as AD.[16] To identify AD-associated DEGs, we applied a cutoff threshold of p value < 0.05 & $|\log_2 FC| > 0.3$ (where FC represents fold change.

Quantitative proteomic analysis was performed on 310 DLPFC samples (110 controls and 200 AD cases) using a tandem mass tag mass spectrometry (TMT-MS) approach. DEPs were identified with an adjusted p value < 0.05 & $|\log_2 FC| > 0.15$ as the significance threshold. To ensure data reliability, proteins lacking Entrez Gene IDs were excluded from subsequent analyses, yielding a final set of high-confidence DEPs.[16]

Drug candidate identification based on DEGs

To identify potential therapeutic drugs for AD, we performed drug-disease association analysis by integrating AD-associated DEGs with small-molecule perturbation profiles from the LINCS database. The analysis employed the RGES to quantify drug-induced transcriptional reversal effects, The computation of RGES was adapted from the previous C-Map method.[14] Drugs with RGES < 0 were considered potential AD therapeutics, as negative RGES values indicate reversal of disease-associated gene expression patterns. A more negative RGES corresponds to a stronger disease-modifying effect, a lower negative RGES indicates higher likelihood to reverse disease gene expression and vice versa.

Drug candidate identification based on DEPs

The C-Map algorithm employs a rank-based on Kolmogorov-Smirnov (KS) statistical approach to identify potential therapeutic compounds by correlating disease gene expression signatures with drug-induced transcriptional profiles.[15] The C-Map analysis generated drug-specific score values, which were subsequently normalized to produce Nscores. Compounds with Nscores > 0 were considered potential therapeutic candidates for AD, as positive Nscore values indicate a reversal of disease-associated gene expression patterns. The

magnitude of the positive Nscore correlates with the strength of this reversal effect, where higher values denoting more pronounced therapeutic potential. Therefore, we selected all small-molecule drugs meeting the Nscore > 0 criterion for further evaluation as potential AD treatments.

BBB and structural similarity for candidate drugs

Small-molecule compounds identified through transcriptomic screening were cross-referenced with proteomics-derived candidates using Venny (VN) diagram analysis (https://bioinformatics.psb.ugent.be/webtools/Venn/). Initially, the BBB permeability of prioritized compounds was predicted with the 'ADMET-AI' in-house module of the SZBC-AI4TCM (https://ai.tasly.com/ui/#/frontend/login). Subsequently, we calculated pairwise structural similarities between compounds using RDKit. Invalid SMILES entries (denoted by -666) and missing values were first removed. Valid SMILES were converted to molecular structures, and RDKit topological fingerprints were generated for each molecule.[17] Tanimoto similarity coefficients were computed for all compound pairs and assembled into a similarity matrix for downstream analysis. The similarity matrix was converted into a tree file using the ape package in R, and the resulting tree was visualized online via the iTOL tool (https://itol.embl.de/).[18] Finally, manual curation of selected compounds was performed to evaluate literature reports, physicochemical properties, toxicity profiles, and commercial availability.

Collection of AD-related targets

We collected AD-related targets from seven databases: Open Targets (https://www.targetvalidation.org/), OMIM (https://omim.org/), GWAS (https://www.ebi.ac.uk/gwas/), MalaCards (https://www.malacards.org/), HGNC (https://www.genenames.org/), GeneCards (https://www.genecards.org/) and 'Disease Target' in-house module of SZBC-AI4TCM (https://ai.tasly.com/ui/#/frontend/login). Common genes present in over two independent databases were systematically identified and retained. After removing the duplicated and protein targets derived from databases were further annotated with a unified symbol name and Homo sapiens Entrez ID according to the National Center for Biotechnology Information (NCBI) Gene database.

Collection of potential drug targets

Targets of drugs were obtained from Pubchem database(https://pubchem.ncbi.nlm.nih.gov/) and ChEMBL database(https://www.ebi.ac.uk/chembl/).[19] And then Targets were collected through Netinfer database(http://lmmd.ecust.edu.cn/netinfer/),[20] which based on Weighted Substructure-Drug-Target Network-Based Inference (wSDTNBI) and Morgan fingerprint, $\alpha = 0.4$, $\beta = 0.2$, $\gamma = -0.5$, $\delta = 20$, $\varepsilon = 4$, 100 targets of predictions for each compound. Finally, combined with manual correction methods, standardize the target names and remove duplicate data to obtain drug target sets respectively.

Drug-disease network construction and pathway enrichment analysis

Venn diagrams were drawn using the online Venny diagram drawing tool (https://bioinformatics.psb.ugent.be/webtools/Venn/), and the network relationships between each drug and AD were constructed using Cytoscape 3.10.2 software. KEGG pathway enrichment analyses and GO analyses were performed on the common targets to obtain the biological processes (BP), cellular components (CC), and molecular functions (MF). The top 10 items of each GO category were visualized by bubble charts for the common targets, and the top 25 pathways from the KEGG enrichment analysis were also visualized to display the data results.

Network proximity analysis

Given Y, the set of disease proteins, T, the set of drug targets and d (x, y), the shortest path length between nodes x and y in the network, which is network proximity. we define:[21]

$$d(X, Y) = \frac{1}{||X||} \sum_{x \in X} \min_{y \in Y} d(x, y)$$

Where, d(x,y) represents the shortest path length between drug targets (x) and disease genes (y). The significance assessment method for drug-disease network proximity is achieved by calculating the z-score through random sampling. During random sampling, the drug targets remain unchanged, while the disease genes are randomly selected such that they maintain the same number and a similar degree distribution as the actual disease genes in the background network. This process is repeated 1000 times. The calculation formula is as follows:

$$z - score = \frac{d - \mu}{\delta}$$

here, μ and δ represent the mean and standard deviation of the drug-disease network proximity obtained through random sampling. A smaller value indicates greater statistical significance (z-score < -1.5 and $p < 0.05$ suggests a significant association between the drug and disease).[21,22]

Statistical analysis

Statistical analyses were expressed as mean ± SD and was performed using GraphPad Prism 9.0 software. Comparisons between two groups were performed using one-way ANOVA. A value of $p < 0.05$ was considered to be statistically significant.

Results

DEGs and DEPs in AD patients

From the gene expression data of 328 DLPFC samples from AD patients (125 control cases and 203 AD cases) sourced from the ROSMAP research organization and the Banner Sun Health Research Institute, genes with a $p\ value < 0.05$ & $|\log_2 FC| > 0.3$ were identified as differentially expressed genes (204 in total), including 117 upregulated genes and 87 downregulated genes.

In the protein expression data of 310 DLPFC samples from AD patients (110 control cases and 200 AD cases), proteins with a corrected p value < 0.05 & $|\log_2 FC| > 0.15$ were selected as significantly differentially expressed proteins. After removing proteins without Entrez IDs, a total of 94 AD-specific differentially expressed proteins were obtained, including 70 upregulated differentially expressed proteins and 24 downregulated differentially expressed proteins.

Drug candidate identification

We integrated the transcriptomic perturbation data of drugs from the LINCS database with 204 DEGs identified from AD patient samples to perform RGES analysis. Following the screening of compounds with RGES < 0 and subsequent removal of duplicates, a total of 688 candidate compounds were obtained. Additionally, we combined the proteomic perturbation data of drugs from the LINCS database with 94 DEPs identified from AD patient samples to conduct C-Map computational analysis. Through this analysis, a total of 7166 candidate compounds were screened based on their connectivity scores.

First, an analysis of the 688 and 7166 candidate compounds was performed, yielding 227 overlapping compounds (Fig. 2A). Leveraging the 'ADMET-AI' in-house module of SZBC-AI4TCM (https://ai.tasly.com/ui/#/frontend/login), the BBB permeability of these compounds and marketed AD drugs was predicted. With the lowest BBB value

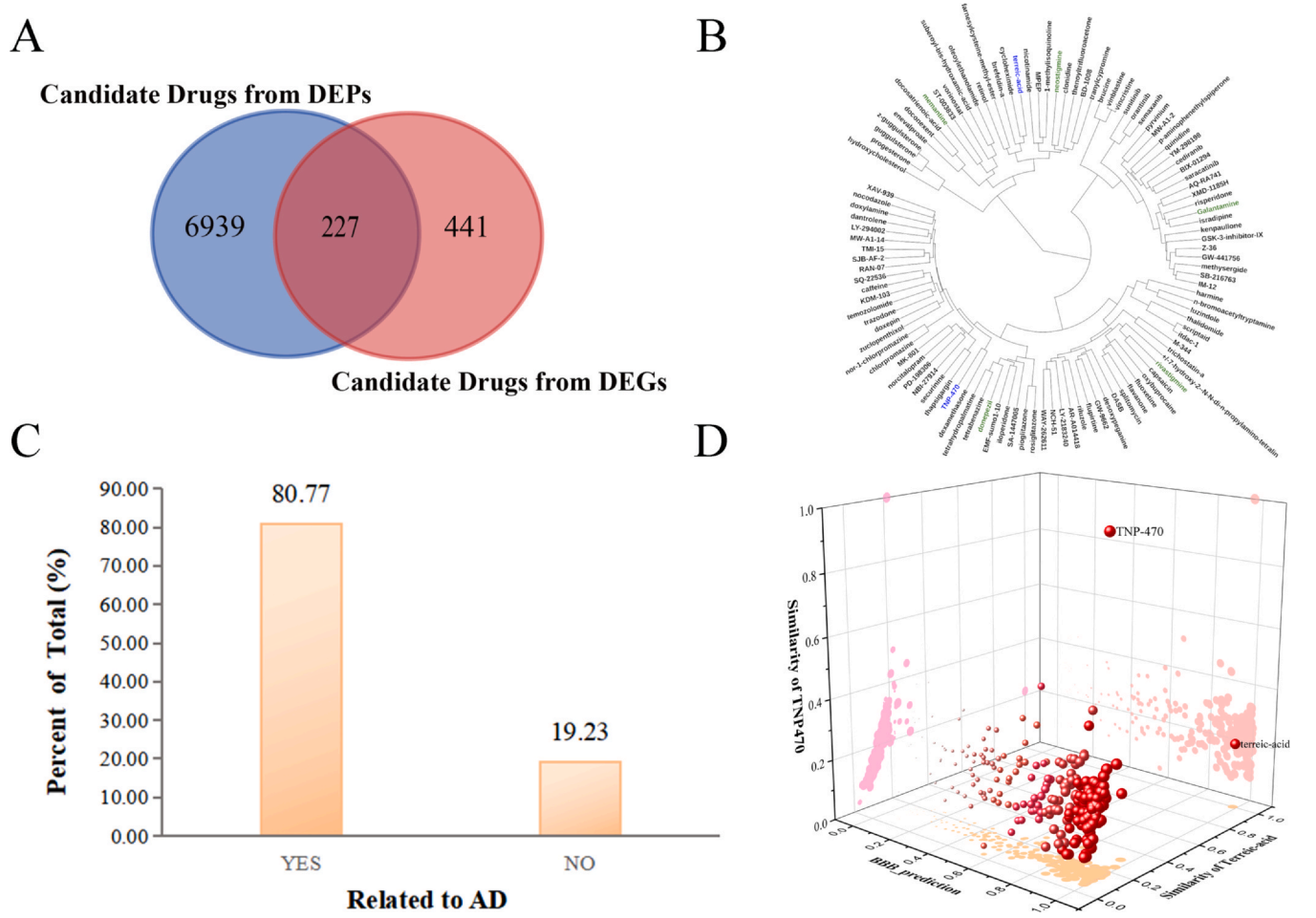

Fig. 2. Screening process of AD Potential drugs. (A) VN Diagram of candidate drugs ; (B) Unsupervised hierarchical clustering of compounds based on the similarity of the chemical structure; the blue-colored text represents the marketed drugs, and the green-colored text represents the screened drugs; (C) AD-related evidence evaluation of the compounds; (D) Comparative structural similarity analysis of compounds TNP-470/Terreic acid and the 104 candidate compounds.

Table 1
BBB prediction scores of marketed drugs in AD.

No.	Name	Smile	BBB_Penetration
1	Donepezil	COC1 = C(C=C2C(= C1)CC(C2 = O)CC3CCN(CC3)CC4 = CC=CC=C4)OC	0.991
2	Memantine	CC12CC3CC(C1)(CC(C3)(C2)N)C	0.990
3	Rivastigmine	CCN(C)C(= O)OC1 = CC=CC(= C1)[C@H](C)N(C)C	0.981
4	Galantamine	CN1CC[C@@]23C=C[C@@H](C[C@@H]2OC4 = C(C=CC(= C34)C1)OC)O	0.971
5	Neostigmine	CN(C)C(= O)OC1 = CC=CC(= C1)[N +](C)(C)C	0.840

among marketed drugs being 0.840 (Table 1), 104 compounds with BBB > 0.840 were filtered, followed by structural similarity analysis (Fig. 2B).

Subsequent literature reviews, patent searches, and report screenings revealed that 84 compounds (80.77 %) had prior AD-related research, while 20 (19.23 %) were unreported, validating the accuracy of our computational approach (Fig. 2C). Two compounds, TNP-470 and Terreicacid, were selected for further analysis. Structural comparisons between these two and the 104 compounds showed low similarity (Fig. 2D), suggesting distinct mechanisms of action for AD treatment compared to existing therapies.

Targets collection of AD and drugs

Disease genes associated with AD were collected from databases. Protein targets were uniformly annotated with official symbol names and gene IDs according to the NCBI Gene database. After manual correction and removal of duplicate genes, a final disease gene set containing 739 unique genes was obtained.

Through systematic database mining and manual curation, including target name standardization (based on NCBI/HGNC guidelines) and redundancy removal, we identified distinct gene sets for each candidate compound: TNP-470 (139 genes) and Terreic acid (102 genes).

Network-based identification of therapeutic pathways

The chemical structure of TNP-470 is illustrated in Fig. 3A. A Venn diagram (Fig. 3B) was generated to compare the target genes of TNP-470 and AD, revealing 40 overlapping genes. A drug-target-disease interaction network was constructed (Fig. 3C), highlighting key molecular relationships. KEGG pathway enrichment analysis of the 40 shared targets identified 32 significantly enriched pathways (adjusted $p < 0.05$). The top 25 pathways, ranked by significance, are displayed in Fig. 3D, including: neuroactive ligand-receptor interaction, lipid and

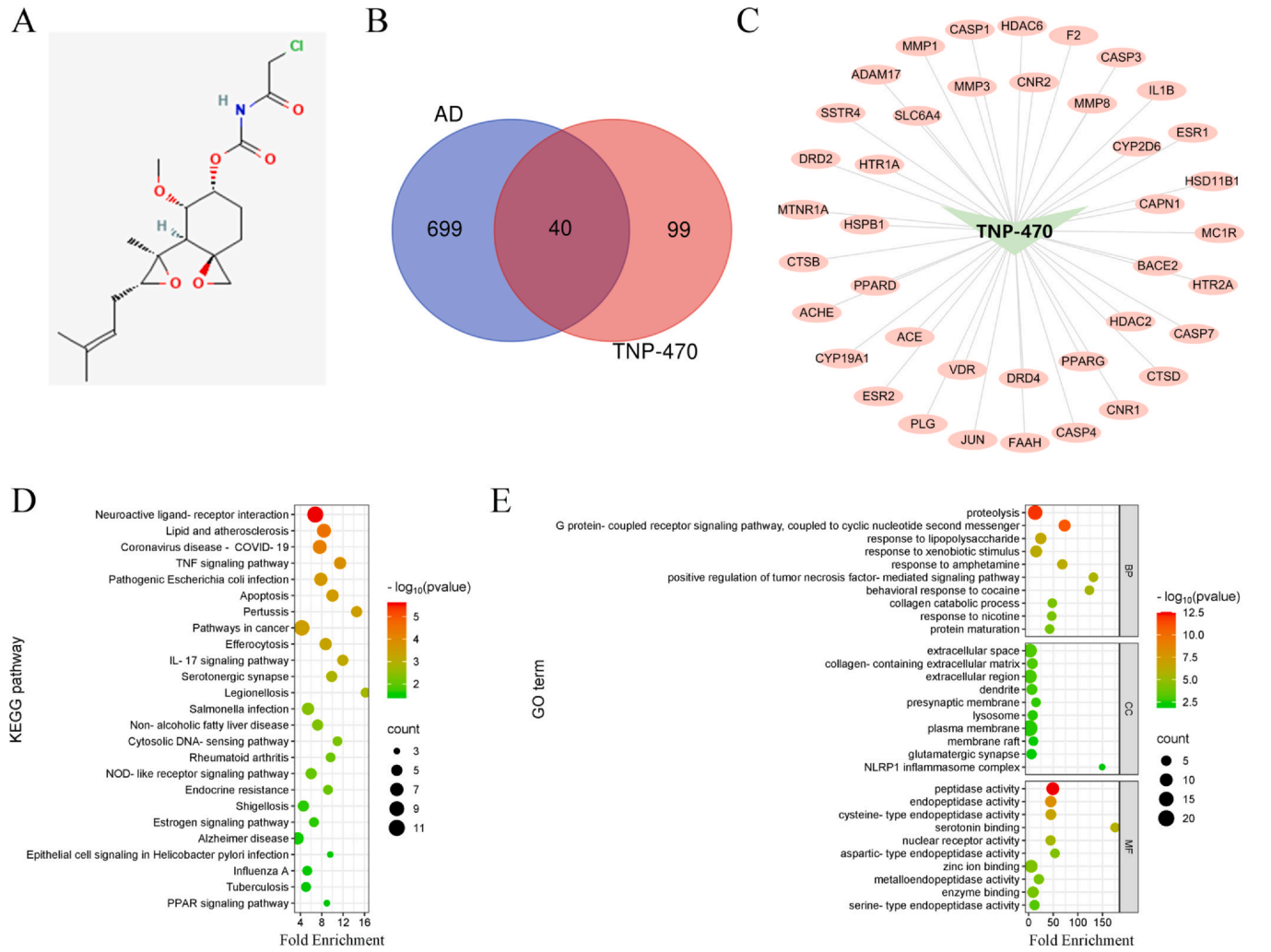

Fig. 3. The analysis of TNP-470 and Alzheimer's disease: (A)The chemical structures of TNP-470; (B)Venn diagram of TNP-470 targets and AD targets; (C) Network of TNP-470 and overlapping targets; (D) KEGG pathway enrichment analysis; (E) GO term enrichment analysis.

atherosclerosis, coronavirus disease, TNF signaling pathway, pathogenic Escherichia coli infection, IL-17 signaling pathway, NOD-like receptor signaling pathway, Endocrine resistance, AD, PPAR signaling pathway, etc. These findings suggest TNP-470 may modulate neuroinflammation, lipid metabolism, and infection-related pathways in AD. GO enrichment analysis further characterized the functional attributes of TNP-470 targets (Fig. 3E). The top 10 significantly enriched terms in each category were as follows: Biological Processes (BP), including proteolysis, G protein-coupled receptor signaling pathway coupled to cyclic nucleotide second messenger, response to lipopolysaccharide, response to xenobiotic stimulus, response to amphetamine, positive regulation of tumor necrosis factor-mediated signaling pathway, behavioral response to cocaine, collagen catabolic process, response to nicotine, and protein maturation, etc; Cellular Components (CC), including extracellular space, collagen-containing extracellular matrix, extracellular region, dendrite, presynaptic membrane, lysosome, plasma membrane, membrane raft, glutamatergic synapse, and NLRP1 inflammasome complex, etc; and Molecular Functions (MF), including endopeptidase activity, cysteine-type endopeptidase activity, serotonin binding, nuclear receptor activity, aspartic-type endopeptidase activity, zinc ion binding, metalloendopeptidase activity, enzyme binding, and serine-type endopeptidase activity, etc. Collectively, these results implicate TNP-470 in neuroprotection, inflammatory regulation, and hormone signaling, with strong associations to AD-relevant mechanisms such as extracellular matrix remodeling, synaptic function, and peptidase-mediated proteolysis.

The chemical structure of Terreic acid is presented in Fig. 4A. Comparative analysis identified 31 overlapping target genes between Terreic acid and AD, as shown in the Venn diagram (Fig. 4B). The interaction network of these shared targets was constructed and visualized in Fig. 4C. KEGG pathway enrichment analysis of the 31 shared targets revealed 21 significantly enriched pathways ($p < 0.05$), with the most relevant pathways illustrated in Fig. 4D: neuroactive ligand-receptor interaction, Serotonergic synapse, calcium signaling pathway, pathways of neurodegeneration, AD, cAMP signaling pathway, gap junction, and others. GO enrichment analysis further characterized the functional attributes of Terreic acid targets (Fig. 4E). The top 10 significantly enriched terms in each category were as follows: BP, including memory, G protein-coupled receptor signaling pathway, positive regulation of synaptic transmission, glutamatergic synaptic transmission, etc.; CC, including presynaptic membrane, postsynaptic membrane, lysosome, plasma membrane, etc.; MF, including peptidase activity, enzyme binding, identical protein binding, nuclear receptor activity, nuclear estrogen receptor activity, protein binding, oxidoreductase activity, etc. These comprehensive analyses demonstrate that Terreic acid primarily modulates pathways related to neurotransmitter systems (particularly dopaminergic and glutamatergic), steroid hormone signaling, and synaptic function. The enrichment in memory-related processes and neurodegenerative pathways suggests that Terreic acid may exert neuroprotective effects through multiple mechanisms relevant to AD pathogenesis. Notably, the compound shows significant involvement in pathways associated with both Alzheimer's and Parkinson's diseases, indicating potential broad-spectrum neuroprotective properties.

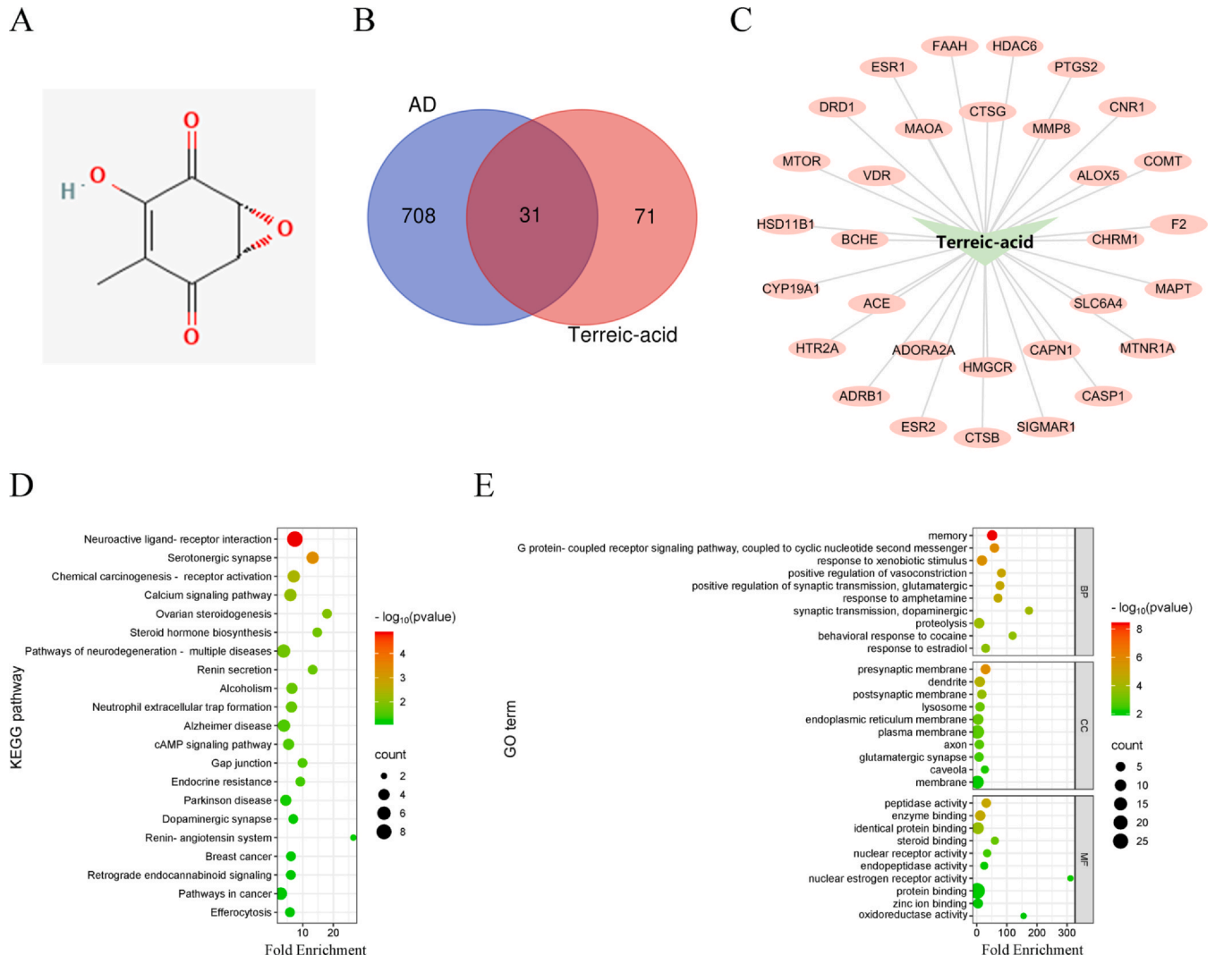

Fig. 4. The analysis of Terreic acid and Alzheimer's disease: (A)The chemical structures of Terreic acid; (B)Venn diagram of Terreic acid targets and AD targets; (C) Network of Terreic acid and overlapping targets; (D) KEGG pathway enrichment analysis; (E) GO terms enrichment analysis.

Calculation of drug-disease association

Using network-based methods, the network proximity between TNP-470 and Terreic acid with AD was calculated respectively. The results showed in Table 2 that, from a network perspective, the target sets of TNP-470 and Terreic acid were in close network proximity to the AD-related gene sets ($p < 0.05$). The z-score values were -8.51 and -8.09, respectively, indicating that TNP-470 and Terreic acid have potential for treating AD.

Results of potential drugs in In vitro experiments

In this study, we employed an OA-induced SH-SY5Y cell injury model and an LPS-induced BV2 cell model to evaluate the pharmacological effects of drugs TNP-470 and Terreic acid.

As shown in Fig. 5, drug TNP-470 exhibited a protective effect against OA-induced SH-SY5Y cell damage at concentrations of 10 μM and 50 μM ($p < 0.01$, $p < 0.001$) (Fig. 5A), significantly improving cell viability. In the LPS-induced BV2 cell model, drug TNP-470 (0.016–10 μM) dose-dependently reduced NO levels (Fig. 5B), suggesting its potential therapeutic benefit in AD.

Fig. 6 shows that drug Terreic acid exerted a concentration-dependent protective effect against OA-induced SH-SY5Y cell injury at 2 μM, 10 μM, and 50 μM ($p < 0.01$, $p < 0.001$, $p < 0.001$, respectively) (Fig. 6A). Meanwhile, drug Terreic acid (10 μM, $p < 0.01$) significantly attenuated LPS-induced BV2 cell damage by reducing NO levels (Fig. 6B). These results suggest that drug Terreic acid may have therapeutic potential for AD.

Table 2
The z-score of network proximity between TNP-470/Terreic acid and AD.

Drug	*z*-score	*p* value
TNP-470	-8.51	0.001
Terreic acid	-8.09	0.001

Discussion

In this study, we successfully integrated drug repositioning strategies with bioinformatics tools to identify and validate potential therapeutic agents for AD. By combining transcriptomic and proteomic data from clinical AD patients, we were able to extract comprehensive disease-related molecular features and screen for DEGs and DEPs. Leveraging the L1000 small-molecule perturbation transcription atlas, we employed two distinct computational methods, RGES and C-Map, to conduct in-depth analyses. Through a reverse scoring system and subsequent comparative analysis, we pinpointed TNP-470 and Terreic acid as promising candidates for AD treatment. Network pharmacology

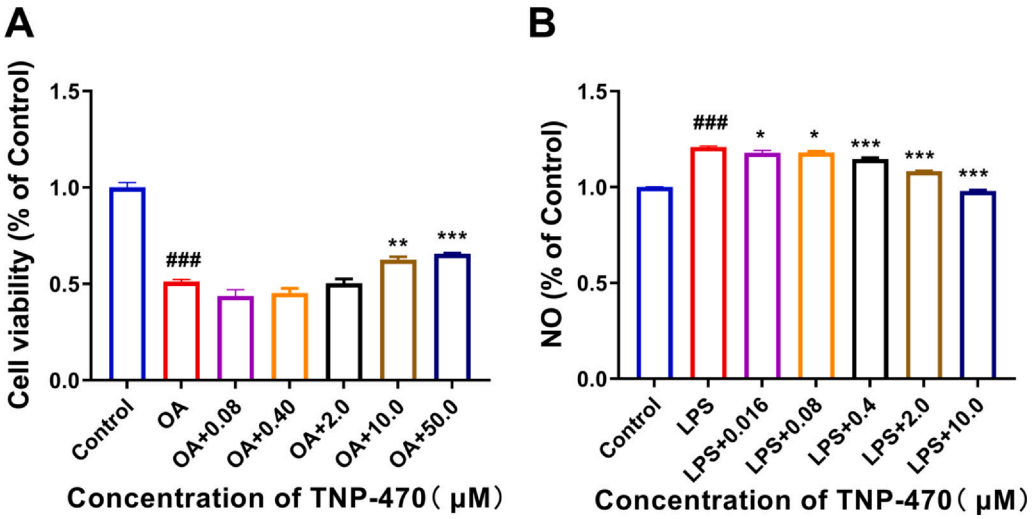

Fig. 5. Experimental results of TNP-470. (A) Viability of OA induced SH-SY5Y cells after treatment with TNP-470 at various concentrations; (B) NO concentration of LPS induced BV2 cells after treatment with TNP-470 at various concentrations. All data are presented as the means ± standard (n = 3) deviations and each experiment was repeated 3 times. Statistical analysis was performed using one-way ANOVA followed by Tukey's post hoc test. ### $p < 0.001$ vs. control group; * $p < 0.05$, ** $p < 0.01$, *** $p < 0.001$ vs. model group.

analysis and network proximity calculations were performed to predict the potential efficacy of these drugs, followed by validation of their pharmacological effects through two independent in vitro cell experiments. Notably, this study utilizes omics data from tissue samples of clinical AD patients and non-AD controls to derive disease-specific expression profiles, providing a more accurate representation of gene expression patterns in real-world patient populations. The integration of multi-omics data and dual drug-screening methodologies enhances the robustness and reliability of the approach, offering a novel framework for AD drug discovery.

TNP-470, as known as AGM-1470 or O-(chloroacetyl-carbamoyl) fumagillol), is a methionine aminopeptidase 2 (MetAP2) inhibitors that enhances the antidiabetic properties of sitagliptin by upregulating xenin.[23,24] Studies have shown that TNP-470 possesses anti-growth factor properties and acts as a potent angiogenesis inhibitor. It can inhibit the activation of cyclin-dependent kinase 2 and the phosphorylation of RB protein, thereby suppressing the formation of new blood vessels in the tumor microenvironment. TNP-470 exhibits inhibitory effects on the in vitro proliferation of multiple tumor cell lines and the growth of solid tumors, with no obvious toxic side effects.[25–27] In the brain tissue of AD patients, persistent angiogenesis occurs in brain regions affected by AD pathology, and it may be associated with tissue damage.[28] If AD is an angiogenesis-dependent disorder, the development of anti-angiogenic drugs targeting abnormal brain endothelial cells may potentially slow AD progression by inhibiting pathological angiogenesis in the AD-affected brain.[29] This study employed network pharmacology analysis and network proximity calculations to predict the association between TNP-470 and AD. Experimental results demonstrated that TNP-470 significantly inhibited OA-induced injury in SH-SY5Y cells and reduced LPS-mediated NO production, thereby exerting protective effects on neuronal cells. Collectively, these findings suggest that TNP-470 may possess therapeutic potential for ameliorating AD pathology.

In postmortem AD brains, microglia surrounding amyloid plaques have been shown to express interleukin-1 (IL-1), a key downstream target in the BTK-associated signaling pathway.[30] Transcriptomic data from both mouse and human brains show that BTK expression is higher in microglial cells compared to other neural cell types[31] Moreover, studies have demonstrated that BTK protein is highly expressed in microglia, and its inhibition using either CC-292 or ibrutinib leads to a reduction in microglial phagocytosis of synaptic structures.[31] This is accompanied by a decrease in overall activation, which is a key feature of neuroinflammatory responses.[32] Terreic acid is an antibiotic metabolite produced by *Aspergillus terreus*. As a quinone epoxide antibiotic, it acts as a Bruton's tyrosine kinase (BTK) inhibitor with anti-inflammatory and antioxidant activities. Terreic acid can inhibit the interaction between protein kinase C (PKC) and the Btk PH (pleckstrin homology) domain.[33] This study predicted the correlation between Terreic acid and AD through network pharmacology analysis and network proximity calculation methods, and identified the anti-AD effects of Terreic acid. Experimental validation showed that Terreic acid could inhibit OA-induced damage in SH-SY5Y cells and reduce LPS-induced

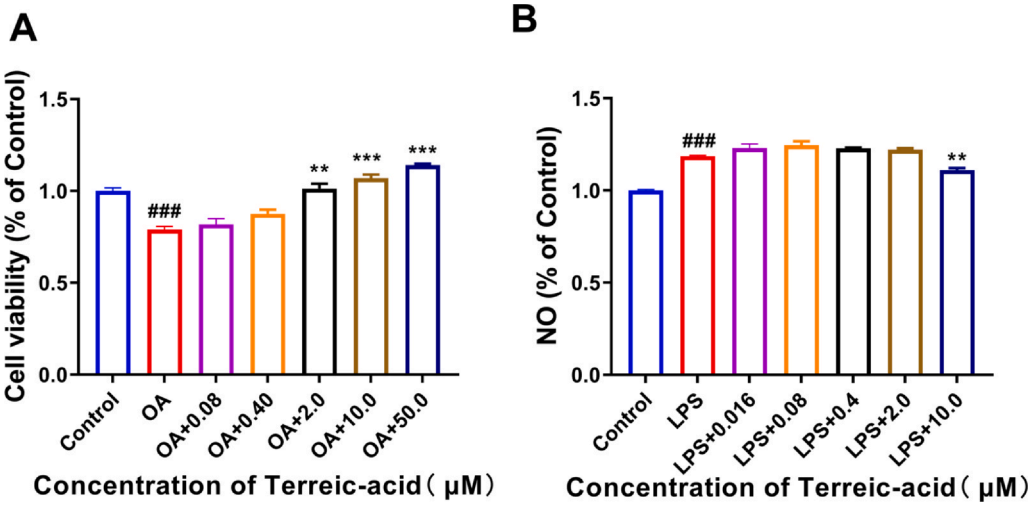

Fig. 6. Experimental results of Terreic acid. (A) Viability of OA induced SH-SY5Y cells after treatment with Terreic acid at various concentrations; (B) NO concentration of LPS induced BV2 cells after treatment with Terreic acid at various concentrations. All data are presented as the means ± standard (n = 3) deviations and each experiment was repeated 3 times. Statistical analysis was performed using one-way ANOVA followed by Tukey's post hoc test. ### $p < 0.001$ vs. control group; ** $p < 0.01$, *** $p < 0.001$ vs. model group.

NO production in BV2 cell models. The results indicate that Terreic acid may possess therapeutic potential for AD.

It is important to acknowledge that AD is a highly heterogeneous neurodegenerative disorder, with pathological changes occurring across multiple.[34] In this study, we focused on the DLPFC, a cortical region critically involved in cognitive control and executive function, which is significantly affected in AD and exhibits robust molecular alterations associated with disease progression.[35–38] However, other key brain regions — such as the hippocampus, entorhinal cortex, and amygdala — are also heavily impacted in early stages of AD and play crucial roles in memory formation and emotional processing. The current analysis was limited to postmortem DLPFC samples due to data availability and prior evidence indicating its relevance in transcriptomic and proteomic studies of AD.[16] While our findings provide valuable insights into potential therapeutic targets in this region, they may not fully represent the molecular landscape or drug response in other affected brain areas. Future studies incorporating multi-regional analyses will be essential to better understand the spatial heterogeneity of AD pathology and to evaluate the broader applicability of identified drug candidates across different brain circuits.

This study introduces a drug repurposing framework that integrates transcriptomic and proteomic data from clinical patients to develop disease-specific expression profiles through multi-omics integration. By utilizing gene expression signatures of drug perturbations and analyzing small-molecule perturbation data from the LINCS database, the approach employs RGES and C-Map scoring algorithms to conduct association analyses for small-molecule repurposing. Potential AD-modulating agents were prioritized through this workflow, which was followed by network pharmacology modeling and network proximity calculations to characterize drug-disease interactomes. Pharmacological validation was subsequently performed using in vitro cell-based assays. This methodology not only establishes an innovative strategy for AD therapeutic discovery but also demonstrates applicability to drug repurposing and de novo drug screening across various disease indications. With the advancement of omics technologies, the expansion of multi-omics repositories, and the exponential increase in biological datasets, the integrative analysis of heterogeneous omics data to construct cross-scale molecular interaction networks is poised to usher in a new era of precision-driven drug repurposing. Future research will aim to extend this framework to combinatorial drug development and improve its mechanistic interpretability, thereby enabling more accurate predictions of drug action pathways.

Conclusion

This drug repositioning strategy, grounded in multi-omics integration, offers an innovative approach to the development of therapeutics for AD. By utilizing gene expression signatures of drug perturbations and analyzing small-molecule perturbation data from the LINCS database, the approach employs RGES and C-Map scoring algorithms to conduct association analyses for small-molecule repurposing, with both TNP-470 and Terreic acid exhibiting potential anti-AD properties.

Declarations

Not applicable.

Authors' contributions

Jinna Yang: Writing – original draft, Visualization, Formal analysis, Data curation. Kaimin Guo: Methodology, Formal analysis. Xiaxia Ren: Methodology, Formal analysis. Xiaolian Zhang: Investigation. Shuang Zhao: Methodology, Formal analysis. Jiansong Fang: Writing – review & editing, Conceptualization. Yu Wei: Writing – review & editing, Conceptualization. Pengcheng Yang: Writing – review & editing, Conceptualization. Wenjia Wang: Writing – review & editing, Conceptualization. Hui Wang: Writing – review & editing, Validation, Funding acquisition. Yunhui Hu: Writing – review & editing, Validation, Funding acquisition.

Ethics approval and consent to participate

Not applicable.

Consent for publication

Not applicable.

Availability of data and materials

Not applicable.

Funding

This research was funded by Tianjin Natural Science Foundation, grant number: 22JCYBJC00180.

Declaration of Competing Interests

The authors declare that they have no known competing financial interests or personal relationships that could have appeared to influence the work reported in this paper.

Acknowledgments

Not applicable.

Authors' other information

Not applicable.

References

1. Long JM, Holtzman DM. Alzheimer disease: an update on pathobiology and treatment strategies. *Cell.* 2019;179(2):312–339.
2. Cummings J, Zhou Y, Lee G, et al. Alzheimer's disease drug development pipeline: 2023. *Alzheimer's Dement (N Y).* 2023;9(2):e12385.
3. GBD 2021. Nervous system disorders collaborators. Global, regional, and national burden of disorders affecting the nervous system, 1990-2021: a systematic analysis for the global burden of disease study 2021. *Lancet Neurol.* 2024;23(4):344–381.
4. Scheltens P, De Strooper B, Kivipelto M, et al. Alzheimer's disease. *Lancet.* 2021;397(10284):1577–1590.
5. Wang G, Qi JL, Liu XY, et al. China Alzheimer report. *J Diagn Concepts Pract.* 2024;23(03):219–256.
6. Beshir SA, Aadithsoorya AM, Parveen A, et al. Aducanumab therapy to treat Alzheimer's disease: a narrative review. *Int J Alzheimers Dis.* 2022;2022:9343514.
7. Cummings J, Apostolova L, Rabinovici GD, et al. Lecanemab: appropriate use recommendations. *J Prev Alzheimers Dis.* 2023;10(3):362–377.
8. Wang H, Pan J, Zhang M, et al. Re-evaluation of the efficacy and safety of anti-Abeta monoclonal antibodies (lecanemab/donanemab) in the treatment of early Alzheimer's disease. *Front Pharm.* 2025;16:1599048.
9. Yu J, Zhao Q, Wang X, et al. Pathogenesis, multi-omics research, and clinical treatment of psoriasis. *J Autoimmun.* 2022;133:102916.
10. Sathyanarayanan A, Mueller TT, Ali Moni M, et al. Multi-omics data integration methods and their applications in psychiatric disorders. *Eur Neuropsychopharmacol.* 2023;69:26–46.
11. Stathias V, Turner J, Koleti A, et al. LINCS data portal 2.0: next generation access point for perturbation-response signatures. *Nucleic Acids Res.* 2020;48(D1):D431–D439.
12. Xie ZJ, Wang J, Han L, et al. Drug repurposing for treatment Alzheimer disease based on LINCS and vesicular glutamate transporter 1 gene sets. *Zhongguo Yaolixue Yu Dulixue Zazhi.* 2022;36(09):641–648.
13. Gao QC, Liu GL, Wang Q, et al. A promising drug repurposing approach for Alzheimer's treatment: givinostat improves cognitive behavior and pathological features in APP/PS1 mice. *Redox Biol.* 2024;78:103420.
14. Chen B, Ma L, Paik H, et al. Reversal of cancer gene expression correlates with drug efficacy and reveals therapeutic targets. *Nat Commun.* 2017;8:16022.
15. Lamb J, Crawford ED, Peck D, et al. The connectivity map: using gene-expression signatures to connect small molecules, genes, and disease. *Science.* 2006;313(5795):1929–1935.

16. Johnson ECB, Carter EK, Dammer EB, et al. Large-scale deep multi-layer analysis of Alzheimer's disease brain reveals strong proteomic disease-related changes not observed at the RNA level. *Nat Neurosci.* 2022;25(2):213–225.
17. Ozturk H, Ozkirimli E, Ozgur A. A comparative study of SMILES-based compound similarity functions for drug-target interaction prediction. *BMC Bioinforma.* 2016;17:128.
18. Letunic I, Bork P. Interactive tree of life (iTOL) v6: recent updates to the phylogenetic tree display and annotation tool. *Nucleic Acids Res.* 2024;52(W1):W78–W82.
19. Wassermann AM, Bajorath J. BindingDB and ChEMBL: online compound databases for drug discovery. *Expert Opin Drug Discov.* 2011;6(7):683–687.
20. Wu Z, Peng Y, Yu Z, et al. NetInfer: a web server for prediction of targets and therapeutic and adverse effects via Network-Based inference methods. *J Chem Inf Model.* 2020;60(8):3687–3691.
21. Cheng F, Desai RJ, Handy DE, et al. Network-based approach to prediction and population-based validation of in silico drug repurposing. *Nat Commun.* 2018;9(1):2691.
22. Wang X, Yang J, Zhang X, et al. An endophenotype network strategy uncovers YangXue QingNao wan suppresses abeta deposition, improves mitochondrial dysfunction and glucose metabolism. *Phytomedicine.* 2024;135:156158.
23. Castronovo V, Belotti D. TNP-470 (AGM-1470): mechanisms of action and early clinical development. *Eur J Cancer.* 1996;32A(14):2520–2527.
24. Craig SL, Gault VA, Flatt PR, et al. The methionine aminopeptidase 2 inhibitor, TNP-470, enhances the antidiabetic properties of sitagliptin in mice by upregulating xenin. *Biochem Pharm.* 2021;183:114355.
25. Kruger EA, Figg WD. TNP-470: an angiogenesis inhibitor in clinical development for cancer. *Expert Opin Invest Drugs.* 2000;9(6):1383–1396.
26. Du L L, Chen Y S, Shi J L, et al. Progress on the antitumor effect of angiogenesis inhibitor TNP-470. *Linchuang Yu Bingli Zazhi.* 2001(01):64–68.
27. Gu JF, Zhang SH. Progress on the antitumor effect of angiogenesis inhibitor TNP-470. *Yaoxue Yu Linchuang Yanjiu.* 2007(04):255–258.
28. Desai BS, Schneider JA, Li JL, et al. Evidence of angiogenic vessels in Alzheimer's disease. *J Neural Transm.* 2009;116(5):587–597.
29. Vagnucci Jr AH, Li WW. Alzheimer's disease and angiogenesis. *Lancet.* 2003;361(9357):605–608.
30. Subramanian J, Savage JC, Tremblay ME. Synaptic loss in Alzheimer's disease: mechanistic insights provided by Two-Photon in vivo imaging of transgenic mouse models. *Front Cell Neurosci.* 2020;14:592607.
31. Keaney J, Gasser J, Gillet G, et al. Inhibition of bruton's tyrosine kinase modulates microglial phagocytosis: therapeutic implications for Alzheimer's disease. *J Neuroimmune Pharm.* 2019;14(3):448–461.
32. Geladaris A, Torke S, Saberi D, et al. BTK inhibition limits microglia-perpetuated CNS inflammation and promotes myelin repair. *Acta Neuropathol.* 2024;147(1):75.
33. Kawakami Y, Hartman SE, Kinoshita E, et al. Terreic acid, a quinone epoxide inhibitor of bruton's tyrosine kinase. *Proc Natl Acad Sci USA.* 1999;96(5):2227–2232.
34. Roemer-Cassiano SN, Wagner F, Evangelista L, et al. Amyloid-associated hyperconnectivity drives tau spread across connected brain regions in alzheimer's disease. *Sci Transl Med.* 2025;17(782):eadp2564.
35. Friedman NP, Robbins TW. The role of prefrontal cortex in cognitive control and executive function. *Neuropsychopharmacology.* 2022;47(1):72–89.
36. Joyce MKP, Uchendu S, Arnsten AFT. Stress and inflammation target dorsolateral prefrontal cortex function: neural mechanisms underlying weakened cognitive control. *Biol Psychiatry.* 2025;97(4):359–371.
37. Yang S, Datta D, Krienen FM, et al. Kynurenic acid inflammatory signaling expands in primates and impairs prefrontal cortical cognition. *bioRxiv.* 2024.
38. Liu A, Manuel AM, Dai Y, et al. Identifying candidate genes and drug targets for Alzheimer's disease by an integrative network approach using genetic and brain region-specific proteomic data. *Hum Mol Genet.* 2022;31(19):3341–3354.